

Supporting information for

**Synergism between iron porphyrin and dicationic ionic liquids: Tandem
CO₂ electroreduction-carbonylation reactions**

Roger Miró,^a Emma Fernández-Llamazares Aragón,^a Cyril Godard,^{c*} Miriam Díaz de los Bernardos,^{a*} and Aitor Gual^{a*}

^a Fundació EURECAT, Unitat de Tecnologia Química, C/Marcel·lí Domingo 2, 43007 Tarragona (Spain)

^c Departament de Química Física i Inorgànica, Universitat Rovira i Virgili, C/Marcel·lí Domingo 1, 43007 Tarragona (Spain).

Table of contents

S1. General conditions	3
S2. Ionic liquid synthesis	4
S2.1. Experimental procedure IL synthesis	4
S2.2. ^1H and $^{13}\text{C}\{^1\text{H}\}$ NMR spectra	6
S3. Description of the electrochemical set-up	8
S4. Description of tandem CO_2 electroreduction and CO utilization set-up	10
S5. Product analysis	12
S4.1. Gas products	12
S4.2. Liquid products.....	14
S5. Metallocoxyolate intermediate formation mechanism	16
S.7. Reduction potentials ($E_{1/2}$) for each IL.....	17
S.8. Effect of the ion-pairing	18
S.9. Graphics under CO_2 for all the IL	19
S.10. Dicationic IL vs. a two-fold concentration of monocationic IL	21
S.11. IL concentration optimization	22
S.12. Current intensity, trifluoroethanol and FeTPP·Cl optimization.....	23
S.13. Tandem CO_2 reduction coupled with Pd-carboxylations	25
S.13.1. Procedure for aminocarbonylation reaction.....	25
S.13.2. Procedure for Sonogashira reaction.....	26
S.13.3. Procedure for alkoxy carbonylation reaction.....	27
S.14. Tandem CO_2 reduction coupled with hydroformylation.....	28
S.15. References.....	31

S1. General conditions

Reagents: Commercially available reagents and solvents were purchased at the highest commercial quality from Sigma-Aldrich, Fisher scientific, Alfa Aesar and were used as received, without further purification, unless otherwise stated.

Analytical methods: ^1H , ^{19}F and $^{13}\text{C}\{^1\text{H}\}$ NMR spectra were recorded using a Varian Mercury VX 400 (400 and 100.6 MHz respectively). Chemical shift values (δ) are reported in ppm relative to TMS (^1H and $^{13}\text{C}\{^1\text{H}\}$), and coupling constants are reported in Hertz. The following abbreviations are used to indicate the multiplicity: s, singlet; d, doublet; t, triplet; q, quartet; quin, quintuplet; m, multiplet; and bs, broad signal.

S2. Ionic liquid synthesis

The monocationic ionic liquids were synthesized following a literature procedure.¹ The dicationic ionic liquids were synthesized following a two steps procedure: (i) preparation of the ionic liquid by mixing at reflux the methylimidazole and the corresponding chlorine precursor to obtain the ionic liquid with the chloride as counter anion. (ii) Then, it is performed the anion exchange with the corresponding salt precursor to obtain the desired ionic liquid.

S2.1. Experimental procedure IL synthesis

General procedure A:

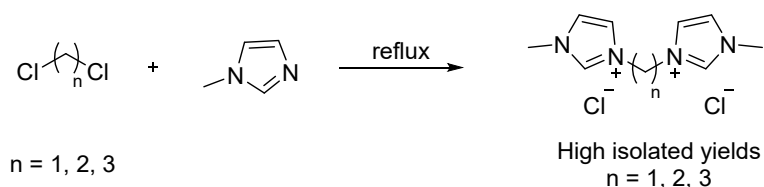


Figure S1: General procedure to synthesize the dicationic ionic liquids with the chloride as counter anion.

According to a modified literature procedure,² a mixture of 2 equivalents of methylimidazole and 1 equivalent of dichloromethane, 1,2-dichloroethane or 1,3-dichloropropane was heated at 90 °C overnight. Then, the reaction was cooled to room temperature and the solid obtained was filtrated and washed with acetonitrile to obtaining the corresponding dicationic ionic liquids with chlorine as counter anion in high isolated yields.

Bis(3-methylimidazolium-1-yl)methane dichloride: Synthesized following a modified literature procedure and obtained as reported in the literature.³ Synthesis performed using 0.36 mol of methylimidazole, IL obtained in a 46% of isolated yield. ¹H NMR (400 MHz, D₂O) δ : 3.97 (s, 6H), 6.70 (s, 2H), 7.60 (d, $J_{\text{H-H}} = 2.0$ Hz, 2H), 7.77 (d, $J_{\text{H-H}} = 2.0$ Hz, 2H).

1,2-Bis(3-methylimidazolium-1-yl)ethane dichloride: Synthesized following a modified literature procedure and obtained as reported in the literature.⁴ Synthesis performed using 1.0 mol of methylimidazole, IL obtained in a 82% of isolated yield. ¹H NMR (400 MHz, D₂O) δ : 3.90 (s, 6H), 4.77 (s, 4H), 7.44 (d, $J_{\text{H-H}} = 2.0$ Hz, 2H), 7.52 (d, $J_{\text{H-H}} = 2.0$ Hz, 2H).

1,3-Bis(3-methylimidazolium-1-yl)propane dichloride: Synthesized following a modified literature procedure and obtained as reported in the literature.⁵ Synthesis performed using 0.2 mol of

methylimidazole, IL obtained in a 74% of isolated yield. $^1\text{H NMR}$ (400 MHz, D_2O) δ : 2.54 (quin, $J_{\text{H-H}} = 6.9$ Hz, 2H), 3.92 (s, 6H), 4.33 (t, $J_{\text{H-H}} = 7.2$ Hz, 4H), 7.49 (s, 2H), 7.53 (s, 2H), 8.80 (s, 2H).

General procedure B:

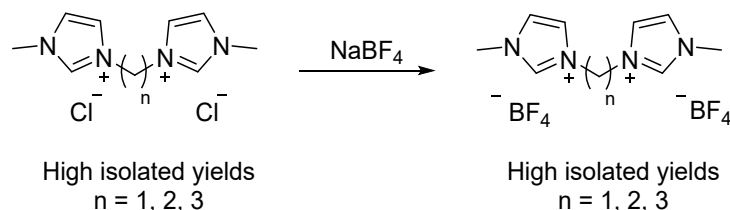


Figure S2: General procedure to perform the anion exchange.

According to a modified literature procedure,⁶ an aqueous solution of the dicationic ionic liquid with the chlorine as counter anion (1 equivalent) and the NaBF_4 (2 equivalents) was stirred at room temperature overnight. Then, the water was evaporated using a rotatory evaporator. The resulting solid obtained was dissolved in acetonitrile, filtered to remove the inorganic salts, and evaporated to obtain the pure ionic liquids with the BF_4^- as counter anion in high isolated yields.

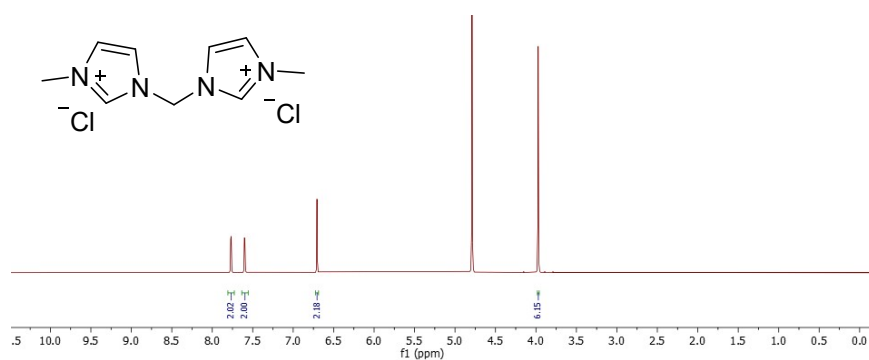
Bis(3-methylimidazolium-1-yl)methane di(tetrafluoroborate) (E5): Synthesis performed using 0.04 mol of Bis(3-methylimidazolium-1-yl)methane dichloride, IL obtained in a 93% of isolated yield. $^1\text{H NMR}$ (400 MHz, $\text{dms}\text{-d}_6$) δ : 3.89 (s, 6H), 6.1 (s, 2H), 7.78 (t, $J_{\text{H-H}} = 1.3$ Hz, 2H), 7.93 (t, $J_{\text{H-H}} = 1.3$ Hz, 2H), 9.32 (s, 2H). $^{13}\text{C}\{^1\text{H}\}$ NMR (100.6 MHz, $\text{dms}\text{-d}_6$) δ : 36.2, 58.2, 121.9, 124.4, 138.0.

1,2-Bis(3-methylimidazolium-1-yl)ethane di(tetrafluoroborate) (E6): Synthesized following a modified literature procedure and obtained as reported in the literature.⁷ Synthesis performed using 0.3 mol of Bis(3-methylimidazolium-1-yl)methane dichloride, IL obtained in a 96% of isolated yield. $^1\text{H NMR}$ (400 MHz, D_2O) δ : 3.90 (s, 6H), 4.76 (s, 4H), 7.44 (t, $J_{\text{H-H}} = 1.8$ Hz, 2H), 7.52 (t, $J_{\text{H-H}} = 1.8$ Hz, 2H), 8.75 (s, 2H).

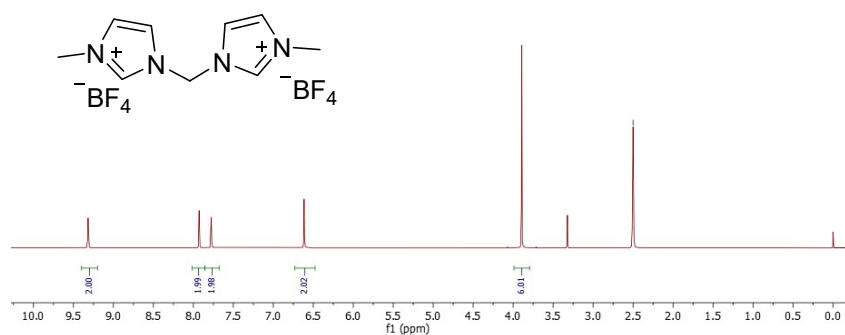
1,3-Bis(3-methylimidazolium-1-yl)propane di(tetrafluoroborate) (E7): Synthesized following a modified literature procedure and obtained as reported in the literature.⁷ Synthesis performed using 0.07 mol of 1,3-Bis(3-methylimidazolium-1-yl)propane dichloride, IL obtained in a 95% of isolated yield. $^1\text{H NMR}$ (400 MHz, D_2O) δ : 2.52 (quin, $J_{\text{H-H}} = 7.4$ Hz, 2H), 3.91 (s, 6H), 4.32 (t, $J_{\text{H-H}} = 7.3$ Hz, 4H), 7.47 (t, $J_{\text{H-H}} = 1.8$ Hz, 2H), 7.50 (t, $J_{\text{H-H}} = 1.8$ Hz, 2H), 8.75 (s, 2H).

S2.2. ^1H and $^{13}\text{C}\{^1\text{H}\}$ NMR spectra

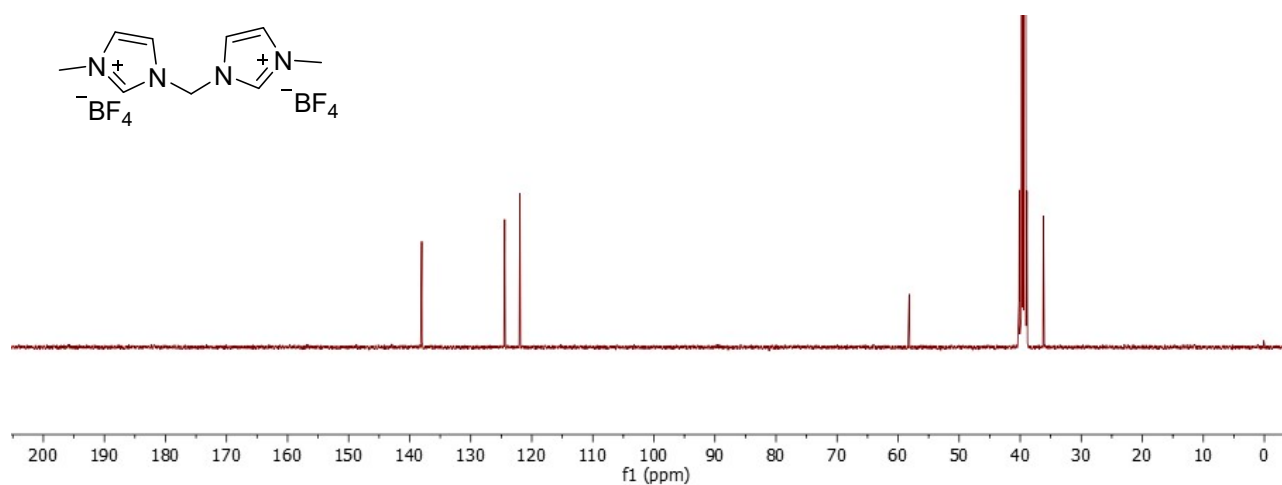
^1H NMR (D_2O , 400 MHz): Bis(3-methylimidazolium-1-yl)methane dichloride



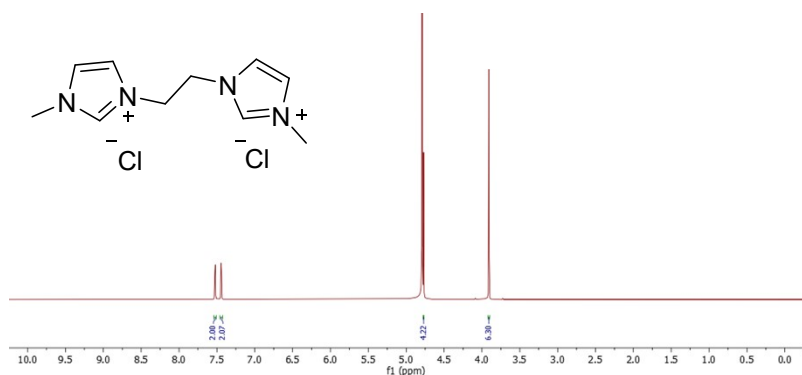
^1H NMR ($\text{dms}\text{-d}_6$, 400 MHz): Bis(3-methylimidazolium-1-yl)methane di(tetrafluoroborate) (E5)



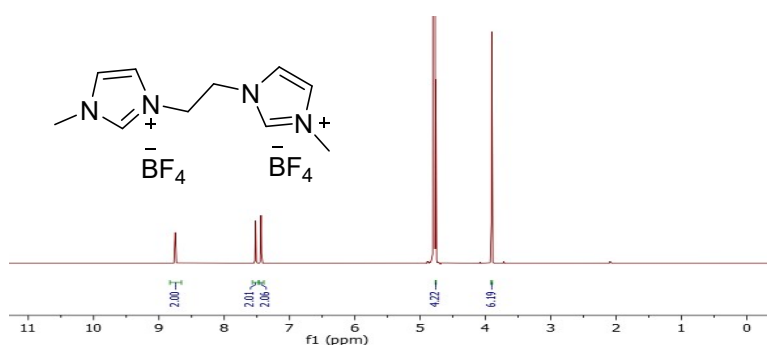
$^{13}\text{C}\{^1\text{H}\}$ NMR ($\text{dms}\text{-d}_6$, 100.6 MHz): Bis(3-methylimidazolium-1-yl)methane di(tetrafluoroborate) (E5)



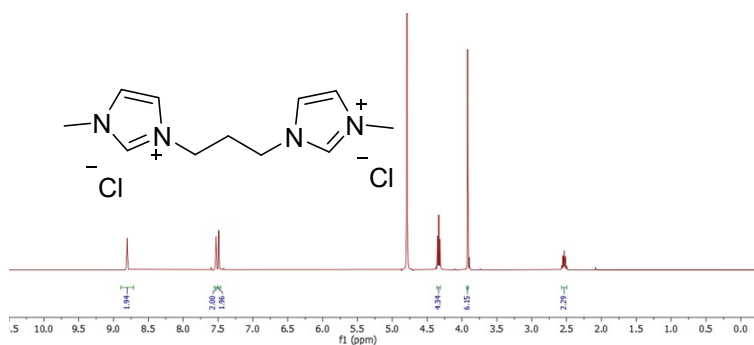
^1H NMR (D_2O , 400 MHz): 1,2-Bis(3-methylimidazolium-1-yl)ethane dichloride



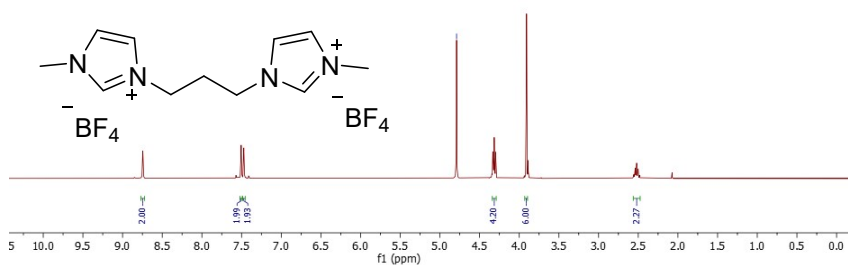
^1H NMR (D_2O , 400 MHz): 1,2-Bis(3-methylimidazolium-1-yl)ethane di(tetrafluoroborate) (E6)



^1H NMR (D_2O , 400 MHz): 1,3-Bis(3-methylimidazolium-1-yl)propane dichloride



^1H NMR (D_2O , 400 MHz): 1,3-Bis(3-methylimidazolium-1-yl)propane di(tetrafluoroborate) (E7)



S.3. Description of the electrochemical set-up

To perform the electrochemical measurements two different cells were used. A smaller cell (**Cell 1**) purchased in bio-logic where was performed the study of the ionic liquids effect and a bigger hand-made cell (**Cell 2**) for the experiments that the gas phase was analyzed. Both cells have a unique chamber. The measurements were performed in a potentiostat form Autolab PGSTAT302N. All potentials in this study were adjusted to NHE reference by adding 0.54 V accordingly to previous measurements with Fc/Fc⁺ as the internal reference. The measurements were performed with and scan rate of 0.1 V·s⁻¹. The reduction CO₂ potential (E^0_{cat}) was measured under CO₂ atmosphere by cyclic voltammetry. The E^0_{cat} refers to the potential at which half of the maximum current is obtained.⁸ All the E^0_{cat} are measured in the same way.

Cell 1: three electrodes configuration cell purchased from bio-logic. In a typical test, the cell was equipped with 0.5 mM of meso-Tetraphenylporphyrin iron(III) chloride (FeTPP), 0.1 M of the corresponding ionic liquid (IL), 1.0 M of trifluoroethanol (TFE) and N,N-dimethylformamide (DMF) as solvent (35 mL). A polished glassy carbon as the working electrode (surface area: 0,07 cm²), platinum wire as a counter electrode, and Ag/AgNO₃ in acetonitrile as reference electrode were used (Figure S3). Prior to each measurement, the electrolyte solution was purged for 20 mins with a nitrogen (N₂) to remove the oxygen present in the solution. Afterwards, the solution was saturated for 1 h under a CO₂ flow.

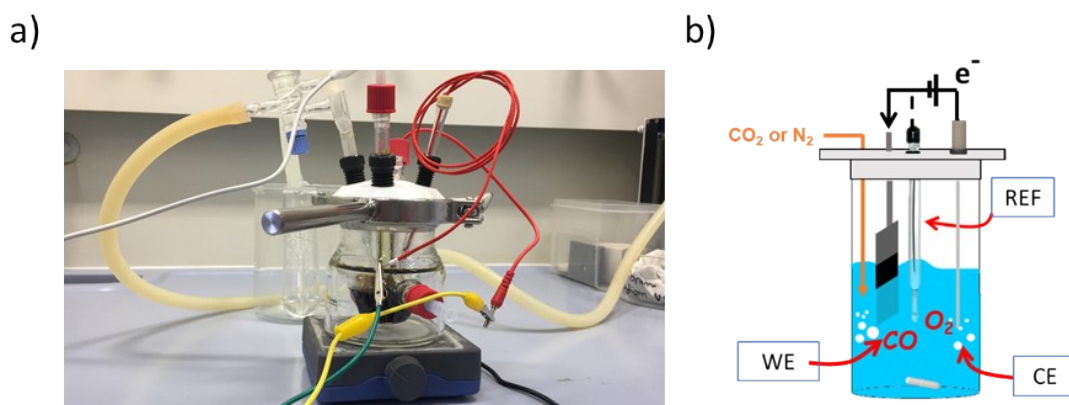


Figure S3: a) Image of the cell 1 and b) schematic representation of cell 1.

Cell 2: Hand-made 3 electrodes configuration cell. In a typical test, the cell was equipped with FeTPP, IL, TFE and 70 mL of DMF, the exact concentrations of FeTPP, IL and TFE are explained in each experiment. A polished glassy carbon as the counter and working electrode (surface area: 9 cm²), and Ag/AgNO₃ in

acetonitrile as reference electrode were used (Figure S4). Prior to each measurement, the electrolyte solution was purged for 30 mins with a nitrogen (N_2) to remove the oxygen present in the solution. Afterwards, the solution was saturated for 2 h under a CO_2 flow.

a)



b)

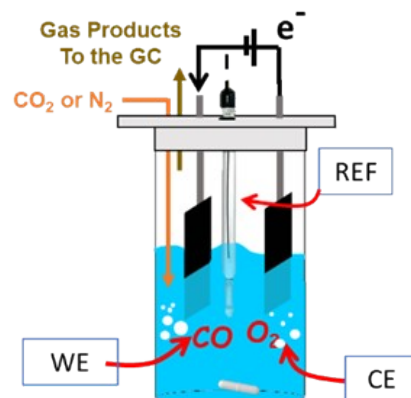


Figure S4: a) Image of the cell 2 and b) schematic representation of cell 2.

S.4. Description of tandem CO₂ electroreduction and CO utilization set-up

To perform the tandem CO₂ electrochemical reduction coupled with carbonylation reaction was used a hand-made cell with two chambers connected between them (Figure S5). In one chamber the CO₂ reduction was performed with a 3 electrodes set-up consisting of a polished glassy carbon as the working electrode (surface area: 9 cm²), a polished glassy carbon as the counter electrode (surface area: 9 cm²) and a reference electrode of Ag/AgNO₃ in acetonitrile. In first chamber a solution of the dicationic-BF₄ ionic liquid (0.3 M), Fe^{III}TPP·Cl (0.8 mM), TFE (1.0 M) in DMF (70 mL) was added, then the solution of this chamber was purged for 20 mins with nitrogen (N₂) to remove the oxygen present in the solution. Afterwards, the solution was saturated for 2 h under a CO₂ flow. Then, a potential of -1.36 V vs NHE was applied during 15h at room temperature and the carbonylation reaction products were analyzed by ¹H NMR using 1,3,5-trimethoxybenzene as internal standard. For the case of the Pd-catalyzed carbonylations, these reactions were performed in the second chamber using 0.5 mmol of the 1-chloro-4-iodobenzene as substrate in presence of the Pd-catalyst and the corresponding reagent for aminocarbonylation, alkoxy carbonylations and Sonogashira process. The detailed conditions are described in the section S12.

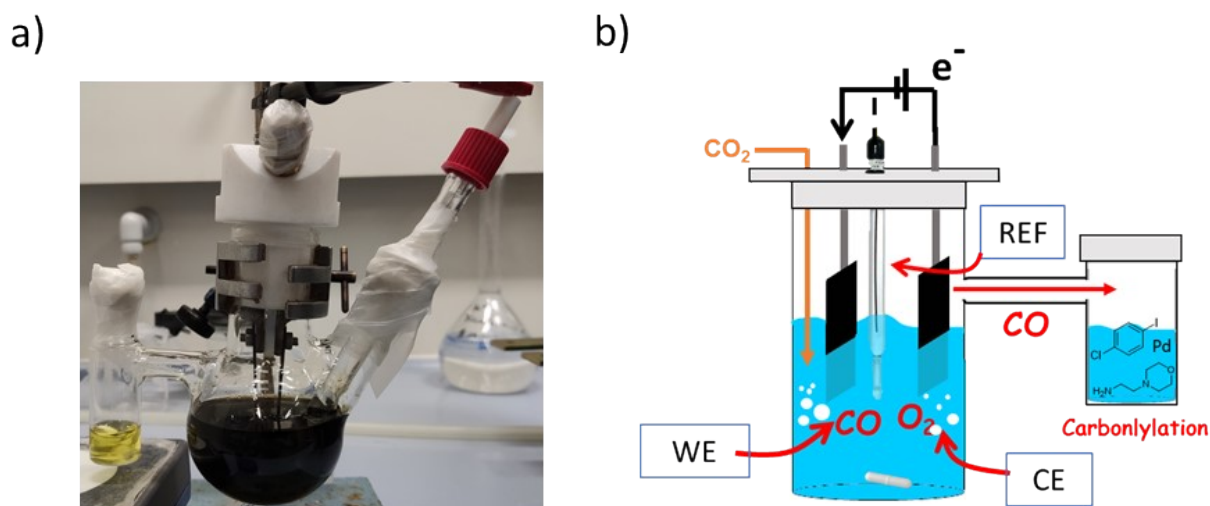


Figure S5: a) Image of the cell used for the tandem reaction and b) schematic representation of the cell.

For the case of the Rh-catalyzed hydroformylation, this reaction was performed by using a simple plastic syringe (24 mL) for transferring the gas generated in (70 mL total death volume with and approximated composition of 0.6 mmol CO and the rest is unreacted CO₂) the electrochemical cell (Cell 2, Figure S4) to a reactor with the THF solution of the Rh-catalyst and 1-octene (0.5 mmol). The transferring procedure is very simple and effective (Figure S6) since only is required to purge the atmosphere of the reactor

(35 mL total volume) with a short vacuum treatment, and later, to fill the reactor 3 times with 24 mL of the gas from the electrochemical cell. Later, the pressure of the reactor system has been corroborated (1.2 bar (gauge)) and hydrogen was added to reach a total pressure of 2.5 bar (gauge), and the reactor was heated at the desired temperature for the selected reaction time. The detailed conditions are described in the section S13.

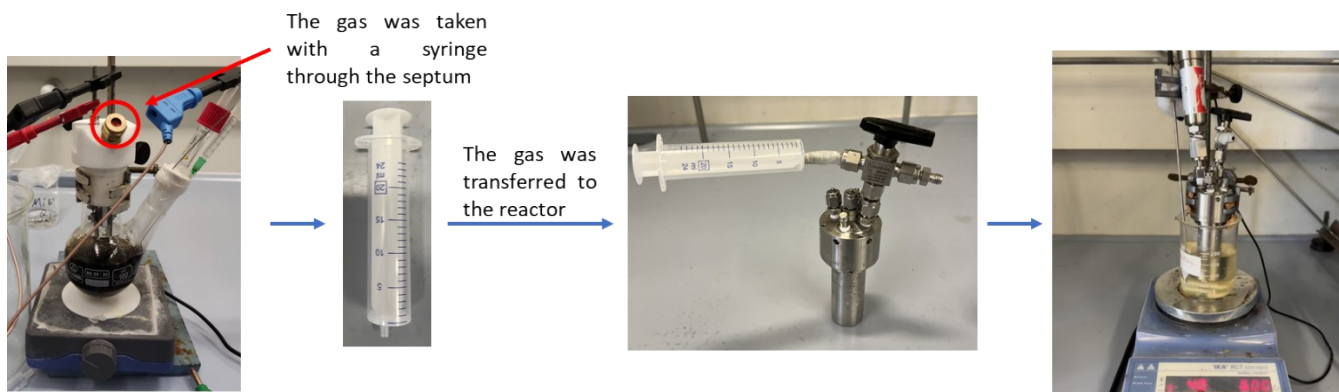


Figure S6: Procedure to perform the tandem CO_2 reduction and Rh-catalyzed hydroformylation reaction of the 1-octene using the autoclave reactor of 25 mL of volume.

S.5. Product analysis

S4.1. Gas products

To analyze the obtained CO and H₂ gas products was used a 500 µL HAMILTON syringe for gas sampling. During the experiment, samples were directly collected at regular intervals and injected (100 µL) in the gas chromatography system (GC System Agilent 7890A with TCD and Agilent 5975C inert MSD with Triple Axis Detection). Gas products were identified/quantified by using calibration curves previous constructed by injecting standard samples of different CO and H₂ concentrations prepared using a home-made system of 3 mass flow controllers (N₂, H₂ and CO).

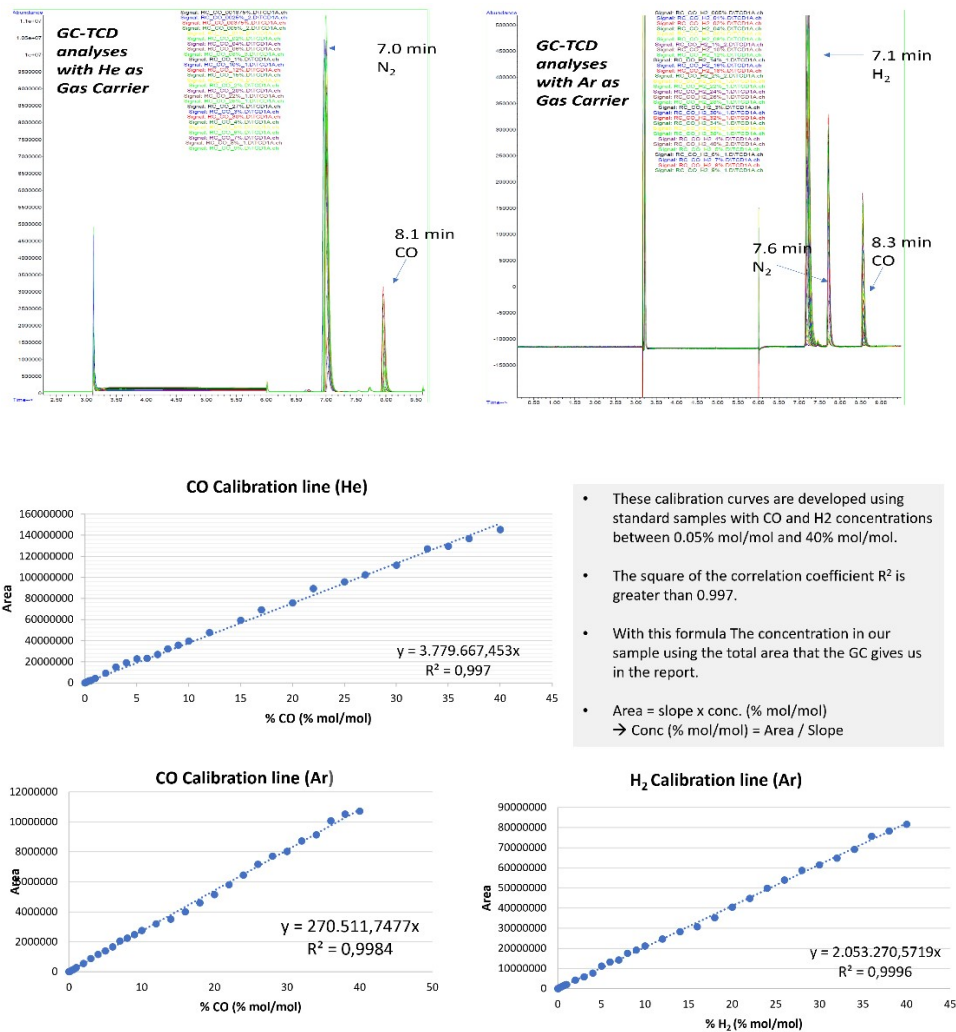


Figure S7: GC-TCD analyses of the standard samples and calibration curves

The CO and H₂ productions were determined by areas obtained from GC-TCD analysis and the response factor obtained from the calibration curves.

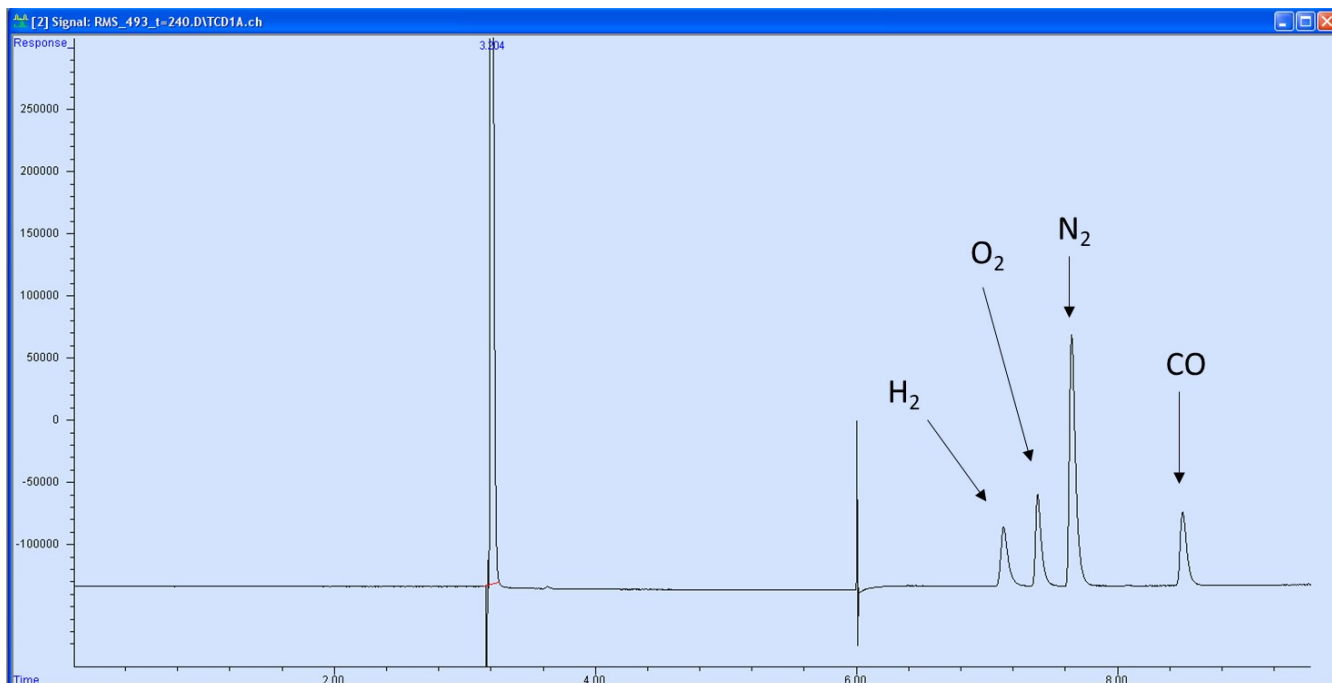


Figure S8: Illustrative example of GC-analyses during an experiment

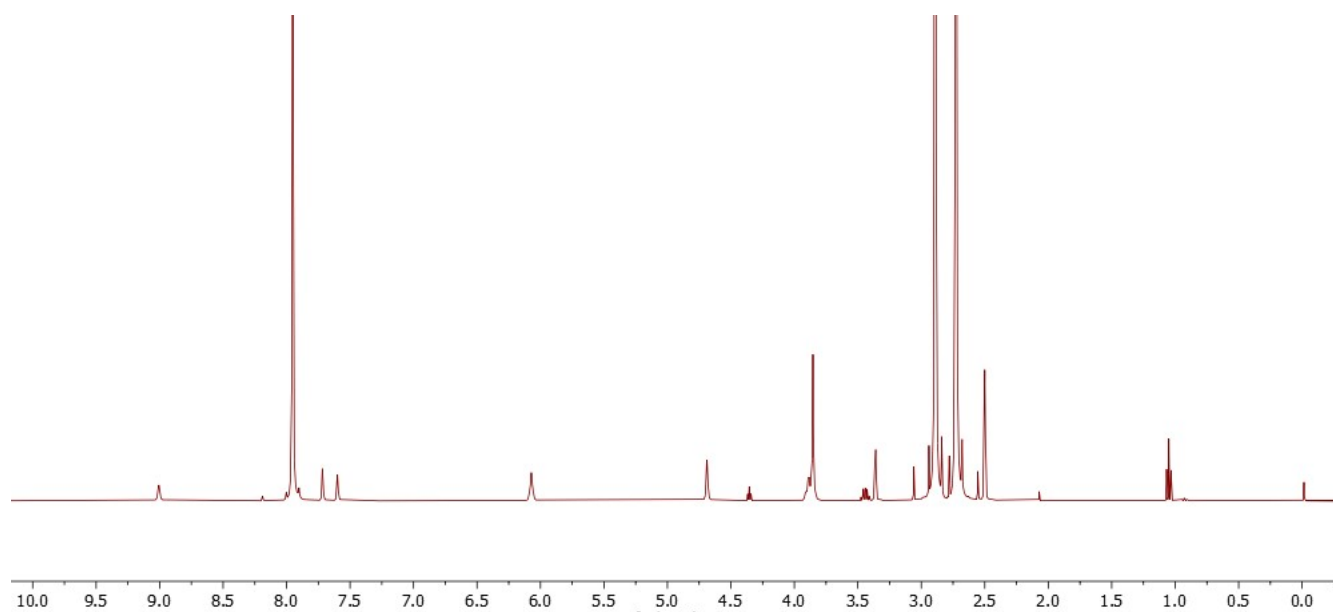
Later, faradaic efficiency (%) of each experiment was calculated using the equation below, where F is the constant of Faraday (96485 C mol^{-1}), Q (C) is the charge passed during the bulk electrolysis, z is the number of moles of electrons required to produce one mole of CO or H₂ from CO₂ or H⁺ and n is the number of moles of product (CO or hydrogen) determined by GC analysis.

$$\text{Faradaic Efficiency (\%)} = \frac{Q_{\text{experimental}}}{Q_{\text{theoretic}}} = \frac{z \cdot n \cdot F}{Q}$$

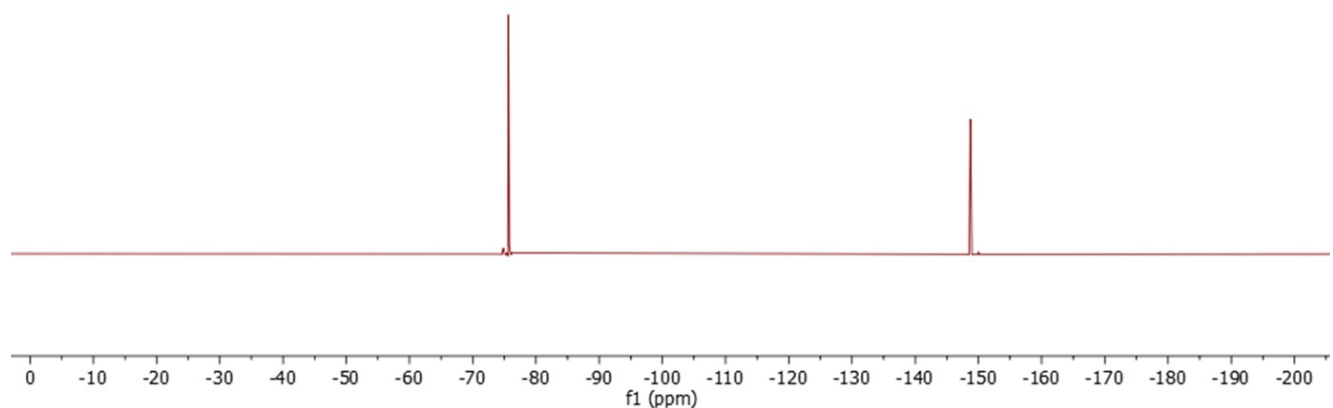
S4.2. Liquid products

The liquid phase was analyzed by taking an aliquot of the solution after the experiment. The aliquot (0.2 mL) was diluted with $\text{dms}\text{-}d_6$ to a total volume of 0.6 mL for its analysis by ^1H , ^{13}C and ^{19}F NMR. The results indicated that: (a) no other CO_2 reduction byproducts (i.e., formate and carbonates) were formed, and (b) the catalyst and the IL are stable under reaction conditions.

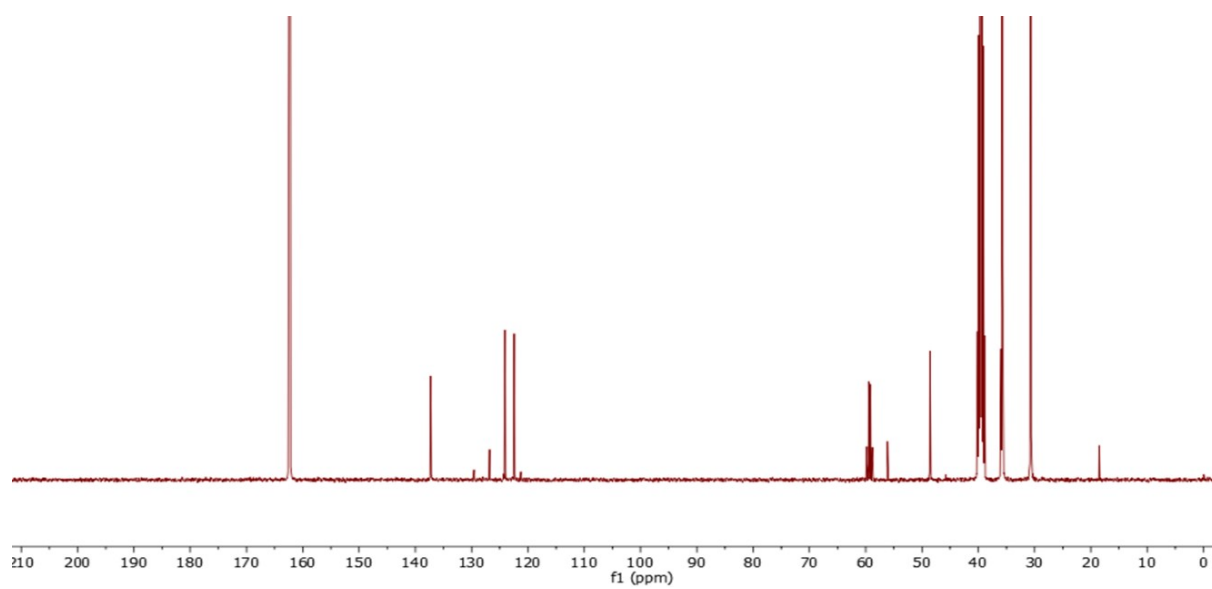
^1H NMR ($\text{dms}\text{-}d_6$, 400 MHz):



^{19}F NMR ($\text{dms}\text{-}d_6$, 400 MHz):

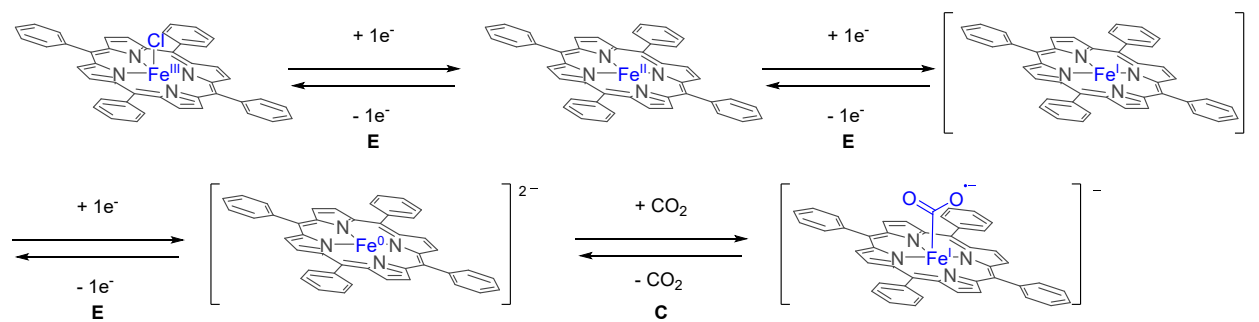


^{13}C NMR (dms o - d_6 , 400 MHz):



S.5. Metalcarboxylate intermediate formation mechanism

a) EEEEC Mechanism in DMF



b) EEC Mechanism in MeCN

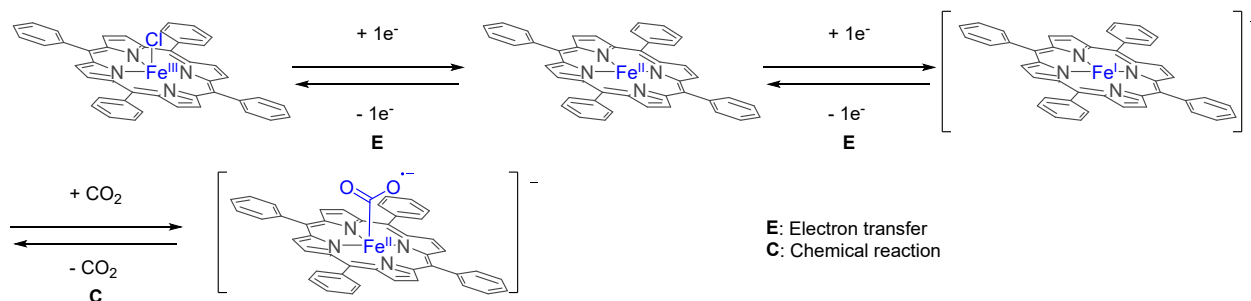


Figure S9: Proposed mechanism for the formation of the metalcarboxylate intermediate of $\text{Fe}^{\text{III}}\text{TPP-Cl}$ a) in DMF via the EEEEC mechanism and b) in acetonitrile via the EEC mechanism. Adapted from ref⁹.

S.7. Reduction potentials ($E_{1/2}$) for each IL

Table S1: Reduction potentials ($E_{1/2}$) of each sample, changing the IL, determined by cyclic voltammetry (V vs. NHE, Scan rate: 100 mV·s⁻¹).
Conditions: FeTPP (0.5mM), TFE (1.0 M), IL (0.1 M), DMF (35 mL) under N₂ or CO₂ atmosphere using cell 1.

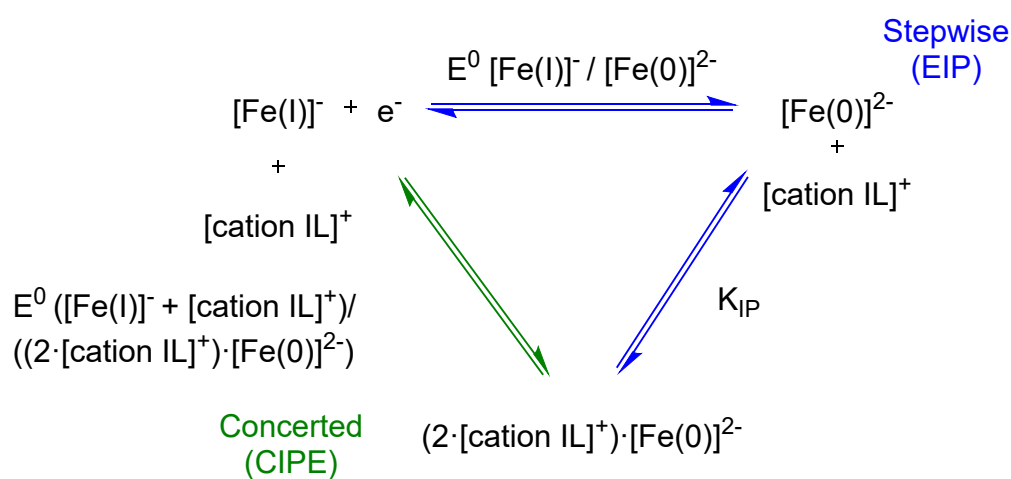
IL	Sample	E Fe ^{III/II}	E Fe ^{II/I}	E Fe ^{I/0}	E ⁰ _{cat}	Overpotential
BMI·BF₄	FeTPP + IL	-0,1	-0,93	-1,43	-1,48	790
	FeTPP + IL + TFE	-0,17	-0,91	-1,4		
BMI·CH₃SO₃	FeTPP + IL	-0,01	-0,94	-1,43	-1,50	810
	FeTPP + IL + TFE	0,01	-0,94	-1,44		
BMI·CH₃COO	FeTPP + IL	-0,2	-1,07	-1,46	-1,50	810
	FeTPP + IL + TFE	-0,25	-0,98	-1,44		
BMI·NTf₂	FeTPP + IL	-0,05	-0,95	-1,45	-1,50	810
	FeTPP + IL + TFE	-0,33	-0,95	-1,43		
BMI·PF₆	FeTPP + IL	-0,5	-0,92	-1,44	-1,49	800
	FeTPP + IL + TFE	-0,33	-0,94	-1,42		
BMI·CF₃SO₃	FeTPP + IL	-0,02	-0,92	-1,43	-1,49	800
	FeTPP + IL + TFE	-0,33	-0,94	-1,42		
BMI·CF₃COO	FeTPP + IL	0,01	-0,95	-1,39	-1,49	800
	FeTPP + IL + TFE	0	-0,94	-1,43		
TBA·PF₆	FeTPP + IL	-0,01	-0,9	-1,54	-1,57	880
	FeTPP + IL + TFE	-0,33	-0,93	-1,53		
TBAPF₆ + BMI·BF₄	FeTPP + IL	-0,09	-0,92	-1,43	-1,50	810
	FeTPP + IL + TFE	-0,18	-0,9	-1,42		
BMMI·BF₄	FeTPP + IL	-0,28	-0,93	-1,5	-1,55	860
	FeTPP + IL + TFE	-0,19	-0,91	-1,49		
EMI·BF₄	FeTPP + IL	-0,02	-0,92	-1,4	-1,49	800
	FeTPP + IL + TFE	-0,3	-0,93	-1,41		
Dicationic·BF₄ n=1	FeTPP + IL	-0,2	-0,43	-0,91	-	-
	FeTPP + IL + TFE	-0,02	-0,42	-0,89		
Dicationic·BF₄ n=2	FeTPP + IL	-0,06	-0,92	-1,33	-1,35	660
	FeTPP + IL + TFE	0	-0,9	-1,31		
Dicationic·BF₄ n=3	FeTPP + IL	0,01	0,98	1,28	-1,34	650
	FeTPP + IL + TFE	0	0,93	1,25		

The electrochemical stability of these ILs has been evaluated by carrying on comparative experiment under nitrogen and under carbon dioxide atmosphere. We corroborated that all the IL electrolytes, except **E5**, are stable under the potential applied since only the iron-catalyst reduction peaks were recorder under nitrogen atmosphere, whereas the experiment under carbon dioxide displayed a

reduction peak around -1.2-1.4 V attributed to the CO₂ reduction to CO. The attribution of this reduction has been carried out by comparing with the related literature and by GC analyzing the gas phase samples collected at regular intervals in order to quantify the formation of CO along the reaction experiment.

Concerning the electrolyte **E5**, this IL displayed under nitrogen atmosphere a reduction peak at more negative potentials than those expected for CO₂ reduction. Under CO₂ atmosphere the same peak was recorded, no CO₂ reduction peak was observed, and GC-analysis confirmed that no CO is being formed under this reaction conditions. Thus, we suspect that the electrolyte **E5** is not stable under the electrochemical potential applied, and it is being decomposed by some process involving reduction steps.

S.8. Effect of the ion-pairing



Scheme S1: Classical stepwise pathways (electron-transfer first, followed by ion-pairing or vice versa), ion-pairing may also occur concertedly with electron transfer.¹⁰

S.9. Graphics under CO₂ for all the IL

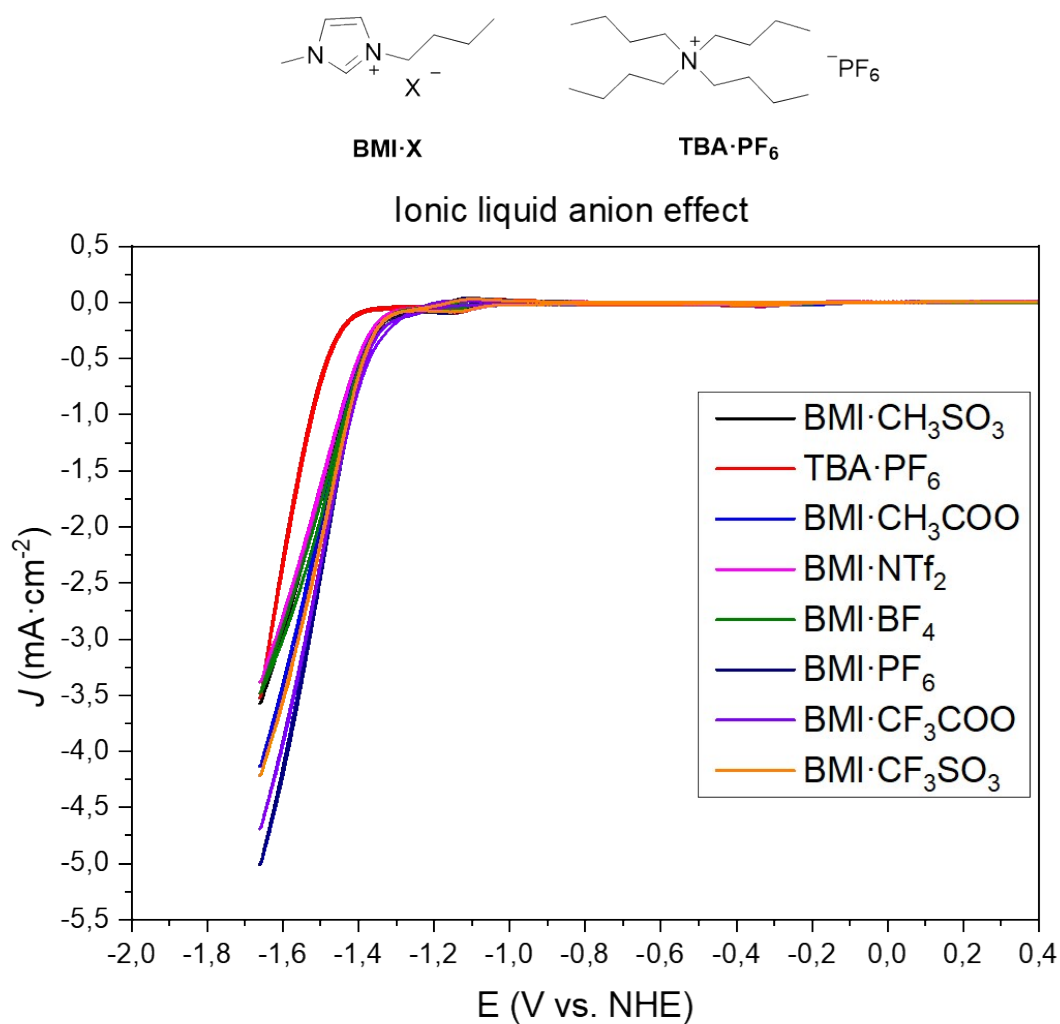


Figure S10: Cyclic voltammetry of different IL changing the anion structure (V vs. NHE, Scan rate: 100 mV·s⁻¹). Conditions: FeTPP (0.5mM), TFE (1.0 M), IL (0.1 M), DMF (35 mL) under CO₂ atmosphere. using cell 1

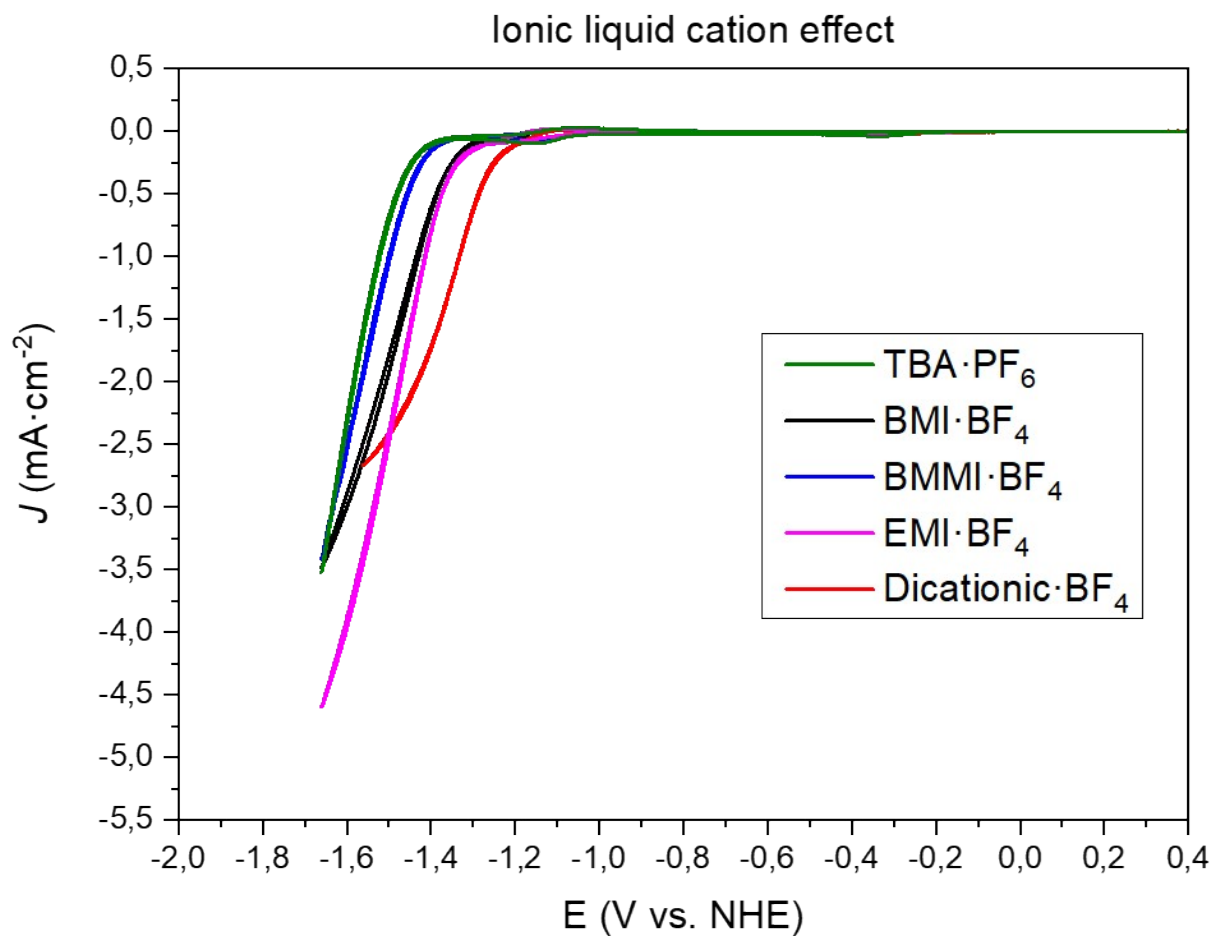
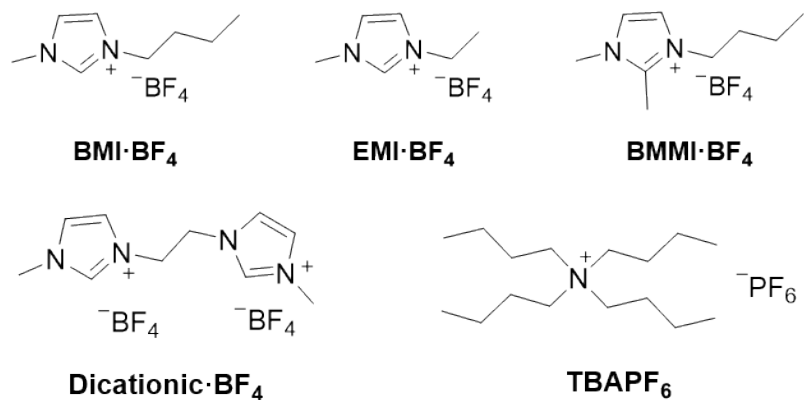


Figure S11: Cyclic voltammetry of different IL changing the cation structure (V vs. NHE, Scan rate: $100\text{ mV}\cdot\text{s}^{-1}$). Conditions: FeTPP (0.5mM), TFE (1.0 M), IL (0.1 M), DMF (35 mL) under CO_2 atmosphere using cell 1.

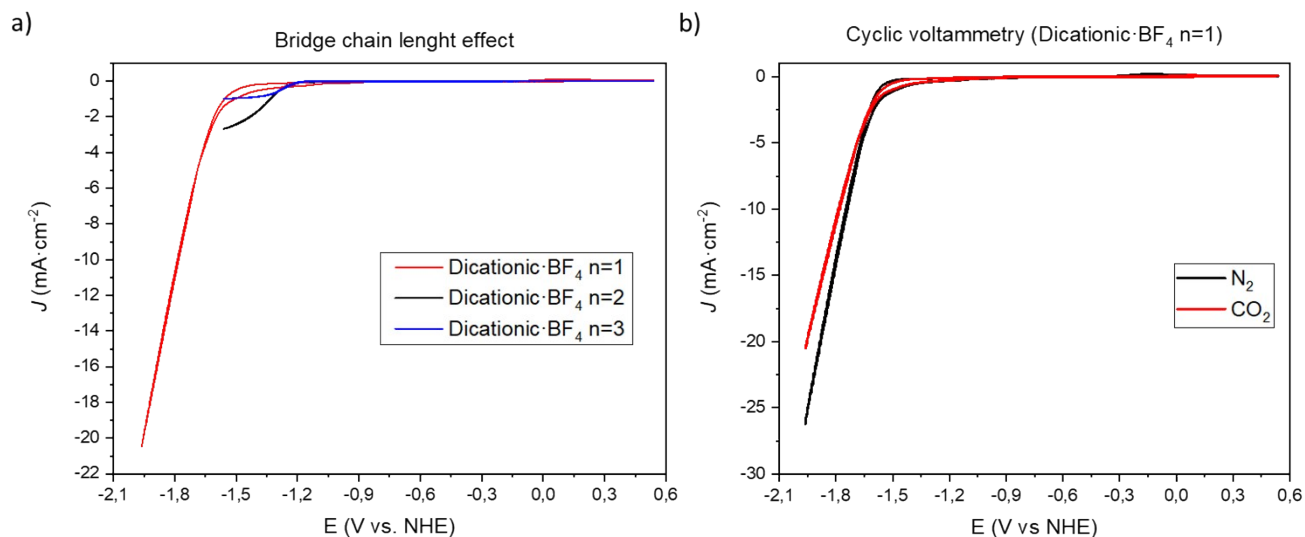


Figure S12: a) Cyclic voltammetry of different IL changing the bridge chain length (V vs. NHE, Scan rate: $100 \text{ mV}\cdot\text{s}^{-1}$). Conditions: FeTPP (0.5 mM), TFE (1.0 M), IL (0.1 M), DMF (35 mL) under CO_2 atmosphere using cell 1. Ionic liquid structures and b) cyclic voltammogram of 0.1 M Dicationic- BF_4 $n=1$, 0.5 mM FeTPPCI, 1.0 M TFE in DMF (35 mL) under N_2 and CO_2 atmosphere using cell 1.

S.10. Dicationic IL vs. a two-fold concentration of monocationic IL

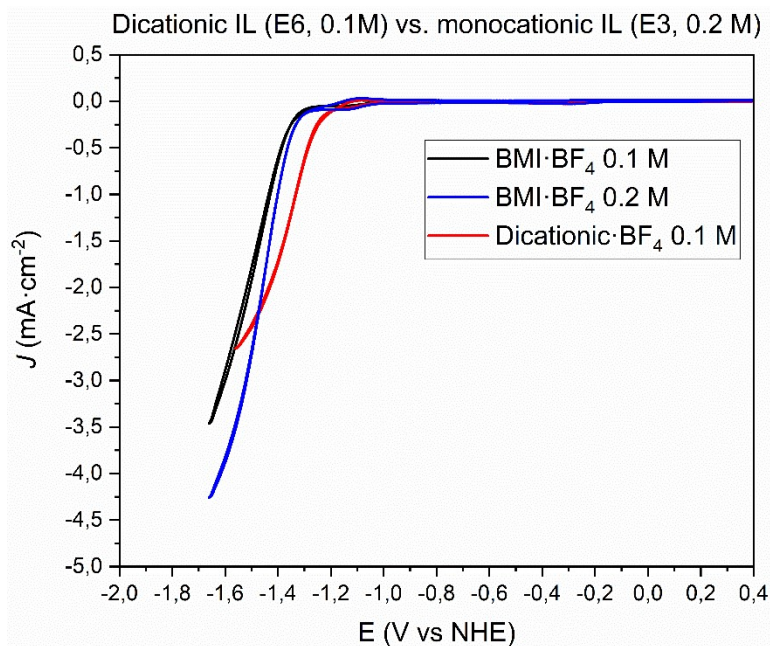


Figure S13: Cyclic voltammogram of 0.5 mM FeTPPCI, 1.0 M TFE varying the ionic in DMF (35 mL) under saturated CO_2 atmosphere using cell 1 (V vs. NHE, Scan rate: $100 \text{ mV}\cdot\text{s}^{-1}$).

S.11. IL concentration optimization

Table S2: Reduction potentials ($E_{1/2}$) of each sample, changing the IL concentration, determined by cyclic voltammetry (V vs. NHE, Scan rate: 100 mV·s⁻¹). Conditions: FeTPP (0.5mM), TFE (1.0 M), IL, DMF (70 mL) under N₂ or CO₂ atmosphere using cell 2.

IL concentration	Sample	E Fe ^{III/II}	E Fe ^{II/I}	E Fe ^{I/0}	E ⁰ _{cat}	Overpotential
0.1 M	FeTPP + IL	-0,06	-0,92	-1,33	-1,40	710
	FeTPP + IL + TFE	0,0	-0,90	-1,31		
0.3 M	FeTPP + IL	-0,02	-0,93	-1,29	-1,33	640
	FeTPP + IL + TFE	-0,03	-0,91	-1,27		
0.6 M	FeTPP + IL	0,02	-0,94	-1,26	-1,25	560
	FeTPP + IL + TFE	-0,03	-0,86	-1,27		
1.0 M	FeTPP + IL	0,03	-0,94	-1,27	-1,24	550
	FeTPP + IL + TFE	0,0	-0,86	-1,26		

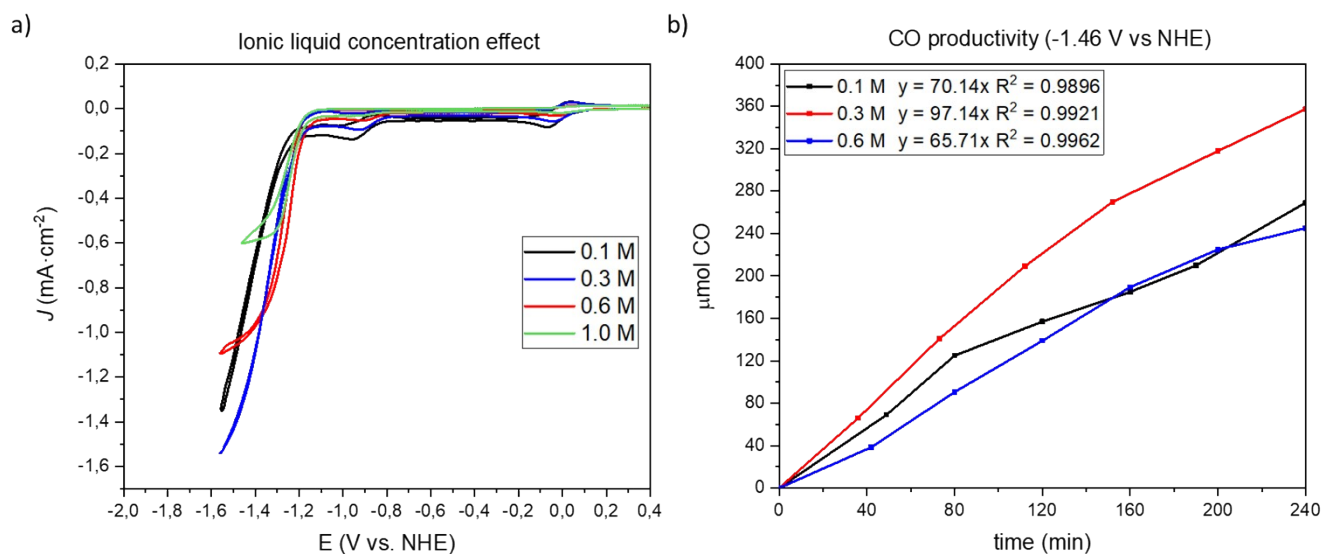


Figure S14: a) Cyclic voltammogram of 0.5 mM FeTPP, 1.0 M TFE varying the dicationic- BF_4 ionic liquid concentration in DMF under saturated CO₂ atmosphere. b) Graphics of CO productivity using different concentration of dicationic- BF_4 ionic liquid. Conditions: 0.5 mM FeTPP, TFE 1.0 M, DMF under saturated CO₂ atmosphere applying -1.46 V vs NHE during 4h.

The effect of IL **E6** concentration (0.1, 0.3, 0.6 and 1.0 M) was evaluated showing that the optimal IL **E6** concentration is 0.3 M as the optimal compromise between more positive $E_{\text{Fe(I)}^-/\text{Fe(0)}^{2-}}$ (-1.31 V to -1.27 V), more positive E^0_{cat} (i.e., from -1.40 V to -1.33 V), higher current density, and maximum CO productivity (0.09 mmol h⁻¹). With 0.1 M and 0.6 M of IL **E6** the CO productivity decrease to 0.07 mmol_{CO}·h⁻¹. At higher **E6** concentrations, a more positive E^0_{cat} is obtained (i.e., from -1.33 V using 0.3 M **E6** to -1.24 V using 1.0 M **E6**).

S.12. Current intensity, trifluoroethanol and FeTPP-Cl optimization

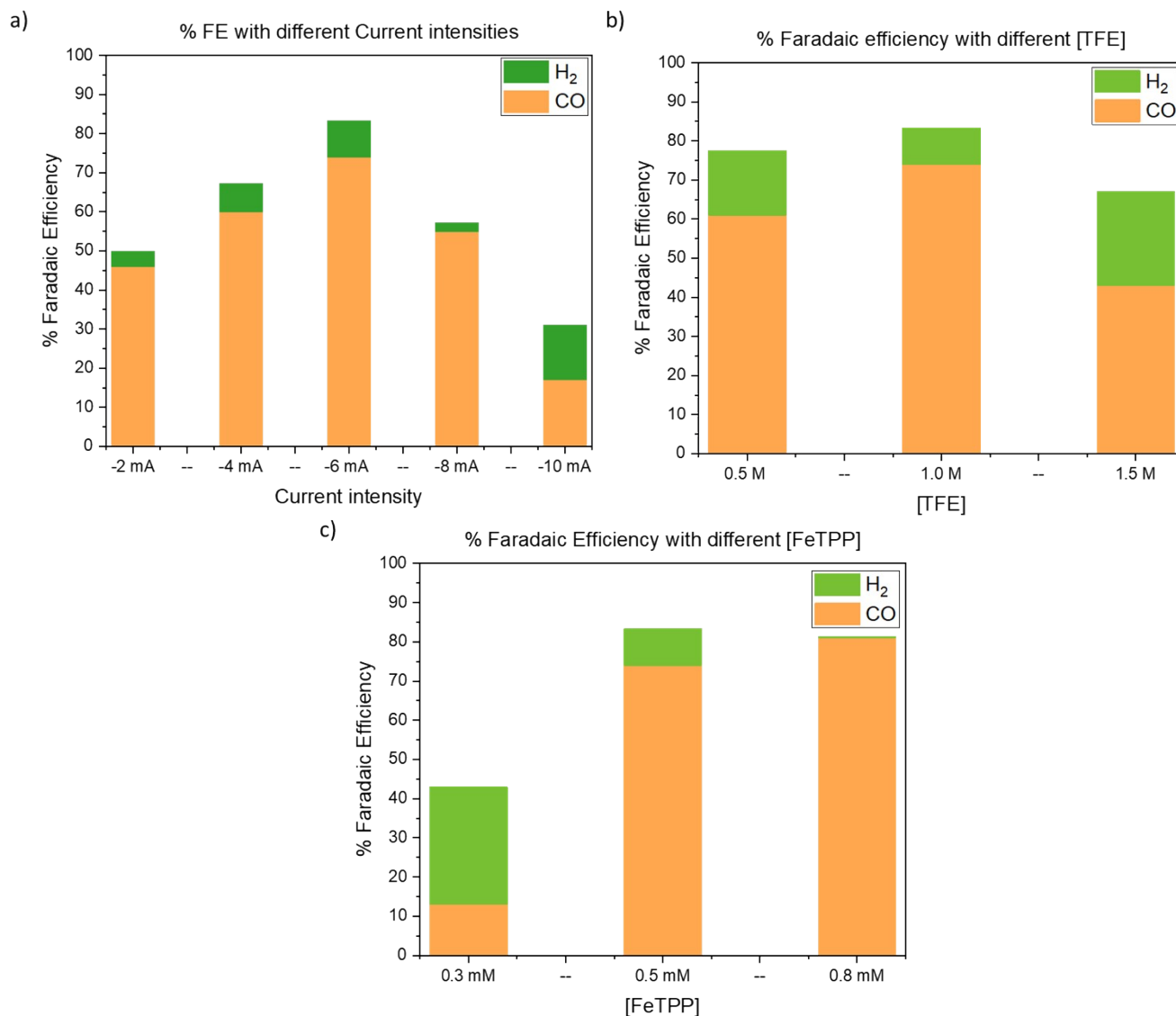


Figure S15: a) % CO and H₂ Faradaic Efficiency applying different current intensities. Conditions: 0.5 mM FeTPP, TFE 1.0 M, 70 mL DMF, 0.3 M dicationic-BF₄ ionic liquid under saturated CO₂ atmosphere applying different current intensities for 4h using cell 2. b) % CO and H₂ Faradaic Efficiency changing the TFE concentration. Conditions: 0.5 mM FeTPP, 70 mL DMF, 0.3 M dicationic-BF₄ ionic liquid under saturated CO₂ atmosphere applying -6 mA for 4h using cell 2. c) % CO and H₂ Faradaic Efficiency changing the FeTPP-Cl concentration. Conditions: 1.0 M TFE, 70 mL DMF, 0.3 M dicationic-BF₄ ionic liquid under saturated CO₂ atmosphere applying -6 mA for 4h using cell 2.

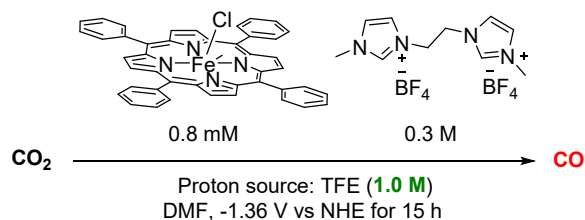
In the current intensity optimization, the highest CO faradaic efficiency (75 %) with a constant production of CO (0.09 mmol·h⁻¹) was obtained by applying current densities of - 6 mA (Figure S15a), with higher or lower current intensities lower Faradaic efficiency values were obtained. With the TFE concentration optimization was observed that the TFE concentration highly affect the rate of CO formation (after 4 h reaction, the CO formation rates are 0.05, 0.09 and 0.05 mmol·h⁻¹ using 0.5, 1.0 and 1.5 M, respectively) and CO/H₂ faradaic efficiencies (61%/17%, 75%/10% and 43%/24% using 0.5,

1.0 and 1.5 M, respectively) (Figure S15b). Finally, was performed the optimization of the **Fe^{III}TPP·Cl** concentration, also showing a clear effect in the CO formation rate (0.01, 0.09 and 0.10 mmol·h⁻¹ using 0.3, 0.5 and 0.8 mM, respectively) and CO/H₂ faradaic efficiencies (13%/30%, 75%/10% and 81%/0.4% using 0.3, 0.5 and 0.8 mM, respectively) (Figure S15c).

A blank experiment was conducted under N₂ atmosphere with the optimized conditions (Conditions: 0.8 mM FeTPP, 1.0 M TFE, 70 mL DMF, 0.3 M dicationic·BF₄ ionic liquid) and a potential of -6 mA for 4 h was applied. The gas phase was analyzed after the 4 hours and any traces of CO was detected.

S.13. Tandem CO₂ reduction coupled with Pd-carboxylations

a) General conditions for CO₂ electrochemical reduction:



b) Different Carbonylations tested in this work:

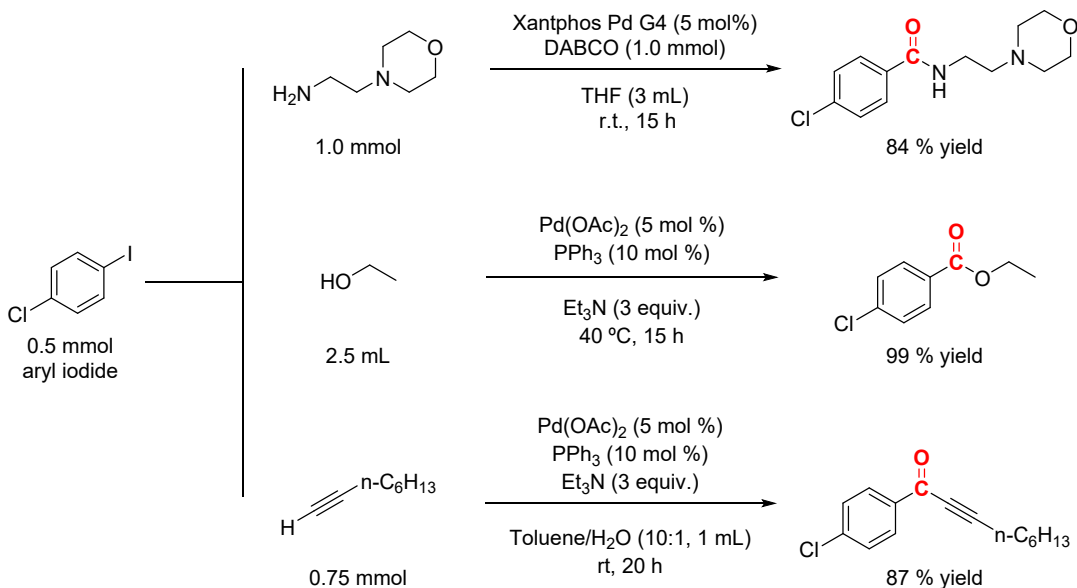


Figure S16: Tandem CO₂ reduction coupled with different Pd-catalyzed carbonylations reactions explored using the two-chamber cell set-up (cell 3).

S.13.1. Procedure for aminocarbonylation reaction

According to a modified literature procedure,¹¹ in a two-chamber reactor (Figure S5) charged with stirring bars 1-chloro-4-iodobenzene (0.5 mmol, 119 mg), 2-morpholinoethylamine (131 μ L, 1 mmol), Xantphos Pd G4 (24 mg, 5 mol%), DABCO (113 mg, 1.0 mmol) and THF (3 ml) were added in the carbonylation chamber. The conditions for the CO₂ reduction chamber are described in the section 0, both chambers were stirred at room temperature. After 15 h applying -1.36 V vs NHE the chemical reaction was analyzed by ¹H NMR using naphthalene as internal standard.

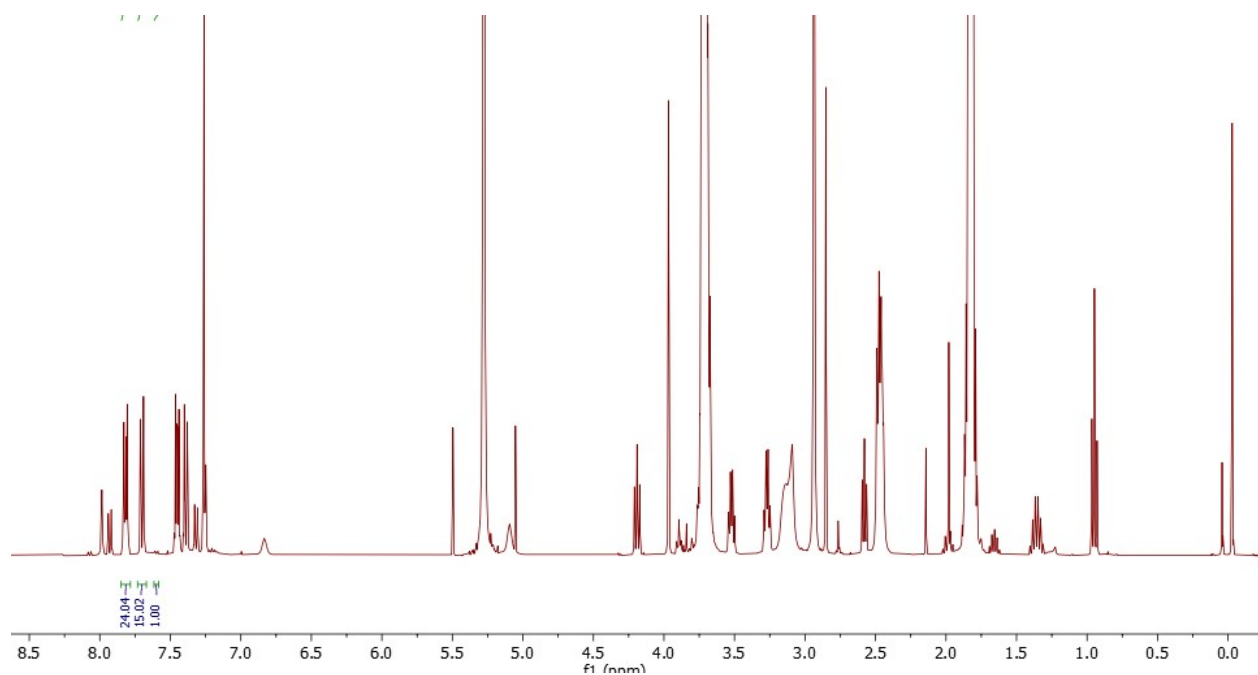


Figure S17: ^1H NMR of the reaction mixture after the reaction. Using naphthalene as internal standard to quantify.

S.13.2. Procedure for Sonogashira reaction

According to a modified literature procedure,¹² in a two-chamber reactor (Figure S5) charged with stirring bars 1-chloro-4-iodobenzene (0.5 mmol, 119 mg), 1-octyne (111 μL , 0.75 mmol), $\text{Pd}(\text{OAc})_2$ (5.6 mg, 5 mol%), PPh_3 (13.1 mg, 10 mol%), Et_3N (209 μL , 1.5 mmol) and Toluene/ H_2O (10:1, 1ml) were added in the carbonylation chamber. The conditions for the CO_2 reduction chamber are described in the section 0, both chambers were stirred at room temperature. The potential was applied during 15 h and the Sonogashira reaction was stirred 5 h more at room temperature. After a total of 20 h the chemical reaction was analyzed by ^1H NMR using 1,3,5-trimethoxybenzene as internal standard.

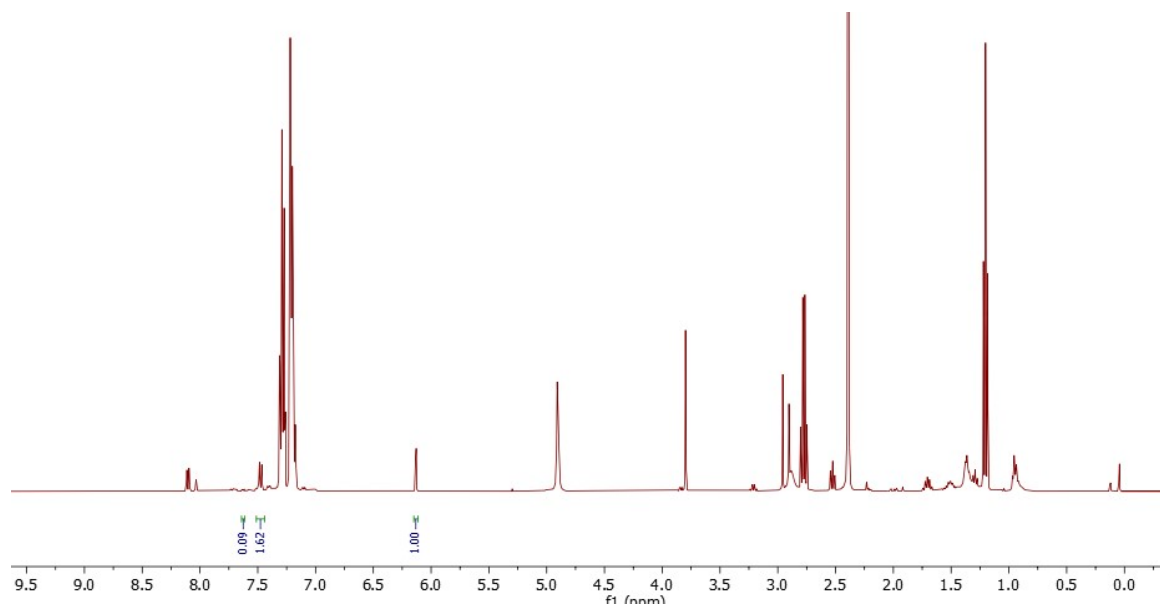


Figure S18: ¹H NMR of the reaction mixture after the reaction. Using 1,3,5-trimethoxybenzene as internal standard to quantify.

S.13.3. Procedure for alkoxycarbonylation reaction

According to a modified literature procedure,¹³ in a two-chamber reactor (Figure S5) charged with stirring bars 1-chloro-4-iodobenzene (0.5 mmol, 119 mg), ethanol (2.5 mL), Pd(OAc)₂ (5.6 mg, 5 mol%), PPh₃ (13.1 mg, 10 mol%) and Et₃N (209 μL, 1.5 mmol) were added in the carbonylation chamber. The conditions for the CO₂ reduction chamber are described in the **section 0**, in this case the carbonylation chamber was stirred at 40 °C while the electrochemical CO₂ reduction chamber was stirred at room temperature. After 15 h applying -1.36 V vs NHE the chemical reaction was analyzed by ¹H NMR using 1,3,5-trimethoxybenzene as internal standard.

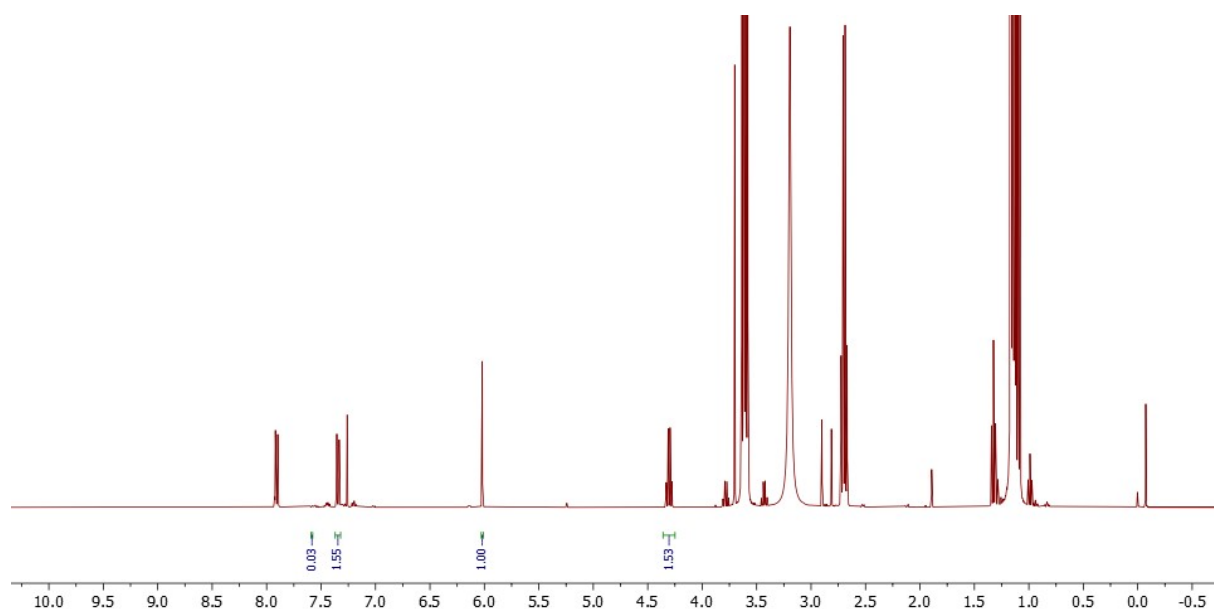


Figure S19: ^1H NMR of the reaction mixture after the reaction. Using 1,3,5-trimethoxybenzene as internal standard to quantify.

S.14. Tandem CO_2 reduction coupled with hydroformylation.

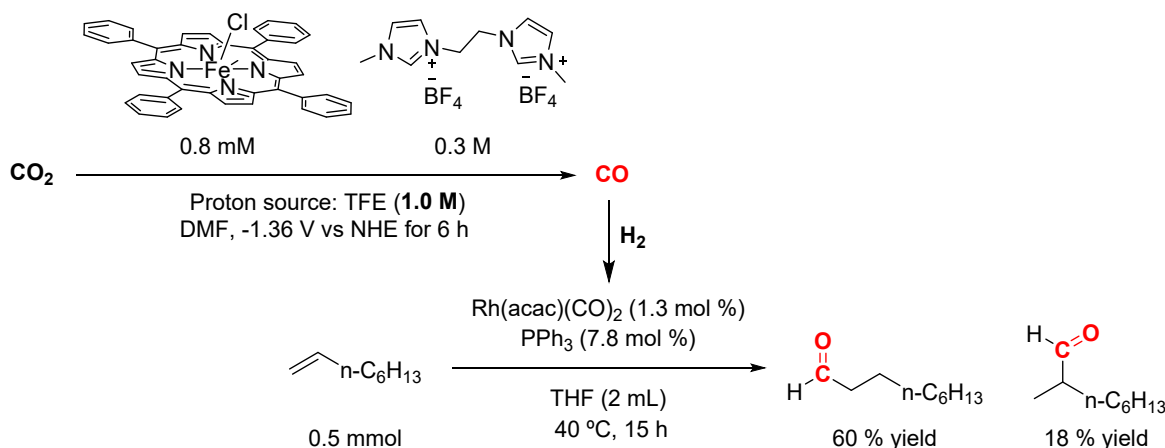


Figure S20: Tandem CO_2 reduction coupled with rhodium-catalyzed hydroformylation of 1-octene

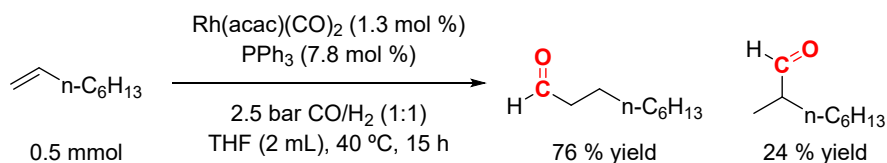


Figure S21: Rh-catalyzed hydroformylation of 1-octene performed using syngas (2.5 bar 1:1 CO/H_2) to compare with the tandem experiment.

To perform the tandem CO_2 reduction coupled with the Rh-hydroformylation a different procedure was followed than for the Pd-carbonylation. In this case, was used the **Cell 2** (Figure S4) to perform the CO_2 electroreduction. The **Cell 2** was equipped with FeTPP (0.8 mM), bicationic- BF_4 IL (0.3 M), TFE (1.0 M) and 70 mL of DMF. A polished glassy carbon as the counter and working electrode (surface area: 9 cm^2), and Ag/AgNO_3 in acetonitrile as reference electrode were used. Prior to perform the bulk electrolysis the electrolyte solution was purged for 30 mins with a nitrogen (N_2) to remove the oxygen present in the solution. Afterwards, the solution was saturated for 2 h under a CO_2 flow. Then, was applied a potential of -1.36 V vs NHE for 6 h.

After the 6 h the gas produced in the **Cell 2** was transferred with a syringe to an auto-clave reactor (Figure S6) of 25 mL of volume (the reactor was under vacuum, the pressure inside the reactor before adding the gas mixture was -0.8 bar gauge) previously charged with octene (0.5 mmol, $78.5\ \mu\text{L}$), $\text{Rh}(\text{acac})(\text{CO})_2$ (1.3 mol %, 1.7 mg), PPh_3 (7.8 mol %, 10.2 mg) and THF (2 ml). After adding the gas produced in the **Cell 2** into the auto-clave reactor, the reactor had a pressure of 1.2 bar gauge, then the reactor was charged until 2.5 bar gauge adding H_2 (1.3 bars of H_2). The hydroformylation reaction was

stirred for 15 h at 40 °C. Finally, the reaction mixture was analyzed by ^1H NMR using 1,3,5-trimethoxybenzene as internal standard.

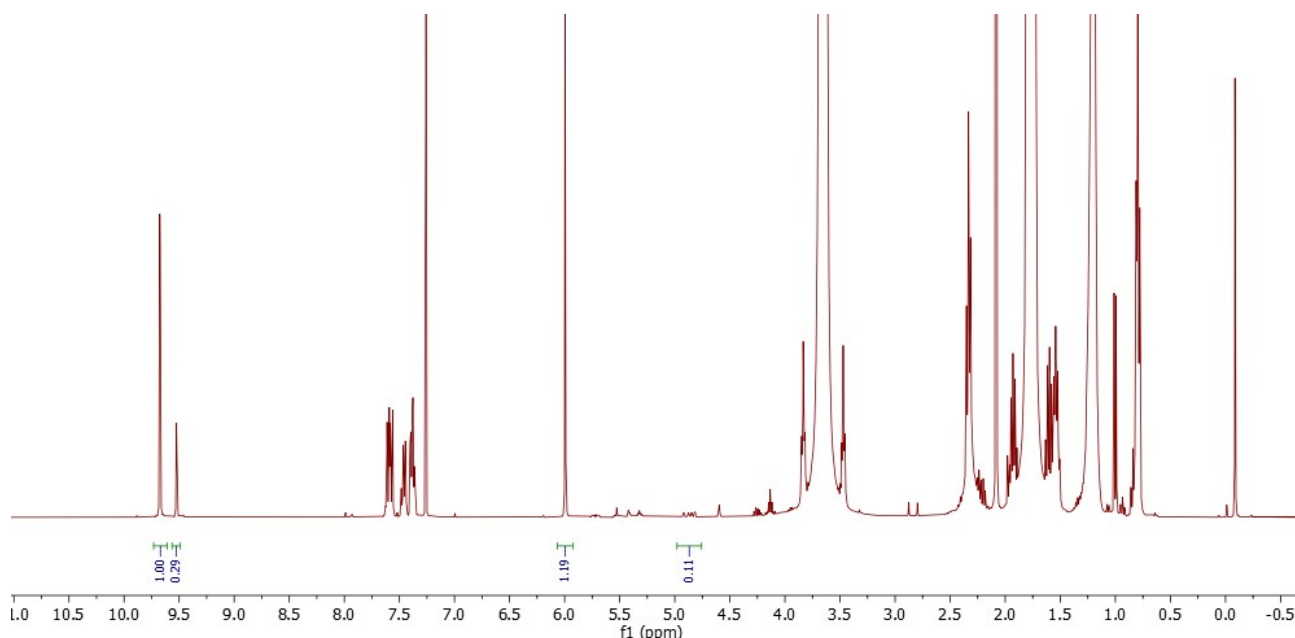


Figure S22: ^1H NMR of the reaction mixture after the reaction with the tandem procedure. Using 1,3,5-trimethoxybenzene as internal standard to quantify.

To compare the results obtained with the Rh-hydroformylation of the 1-octene using the tandem procedure a Rh-catalyzed hydroformylation using a syngas mixture (1:1 CO/H_2) was performed. The auto-clave reactor (25 mL of volume) was charged with octene (0.5 mmol, 78.5 μL), $\text{Rh}(\text{acac})(\text{CO})_2$ (1.3 mol %, 1.7 mg), PPh_3 (7.8 mol %, 10.2 mg) and THF (2 ml). Then, the reactor was charged until 2.5 bar using a syngas mixture (1:1 CO/H_2). The hydroformylation reaction was stirred for 15 h at 40 °C. Finally, the reaction mixture was analyzed by ^1H NMR using 1,3,5-trimethoxybenzene as internal standard. With the syngas mixture higher conversion was obtained with similar selectivities compared with the tandem procedure.

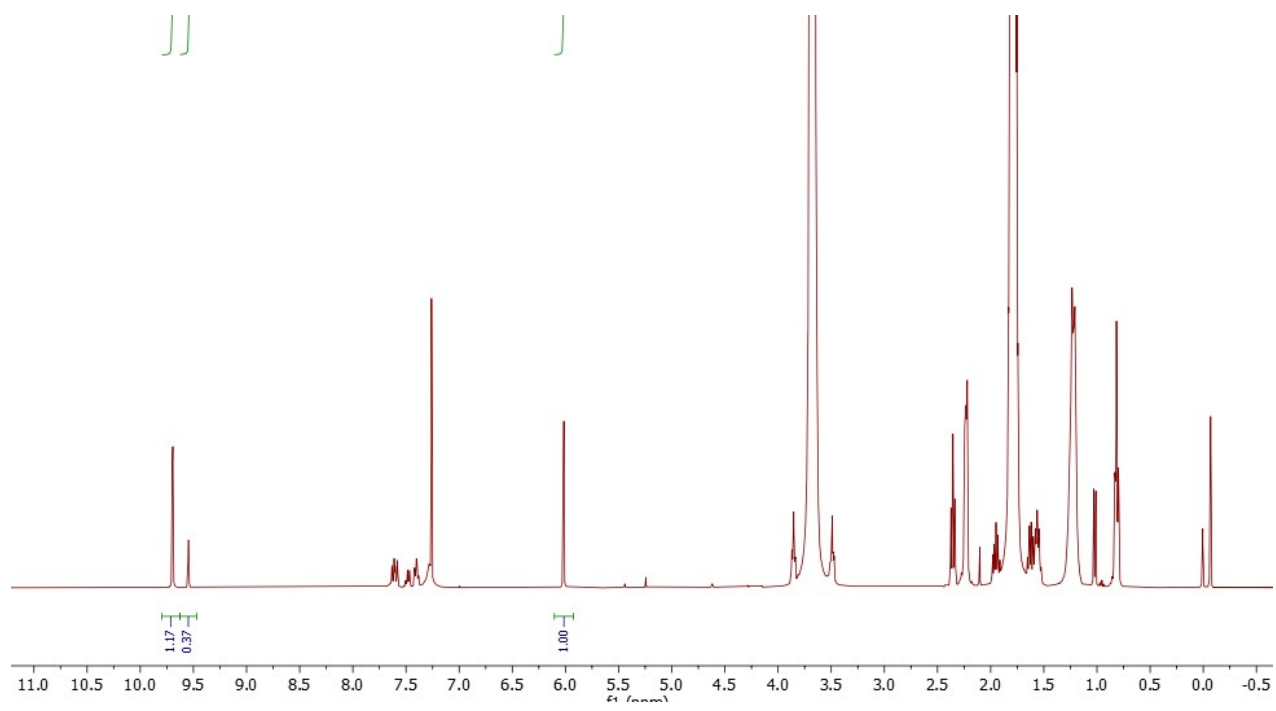


Figure S23: ^1H NMR of the reaction mixture after the reaction using a syngas mixture. 1,3,5-trimethoxybenzene was used as internal standard to quantify.

S.15. References

- (1) Dupont, J.; Consorti, C. S.; Suarez, P. A. Z.; Souza, R. F. de. Preparation of 1-Butyl-3-Methyl Imidazolium-Based Room Temperature Ionic Liquids. *Org. Synth.* **2003**, pp 236-236. <https://doi.org/10.1002/0471264180.os079.28>.
- (2) Nachtigall, F. M.; Corilo, Y. E.; Cassol, C. C.; Ebeling, G.; Morgon, N. H.; Dupont, J.; Eberlin, M. N. Multiply Charged (Di-)Radicals. *Angew. Chem. Int. Ed.* **2008**, *47* (1), 151–154. <https://doi.org/10.1002/anie.200703858>.
- (3) Fernández, A.; Vázquez-García, D.; García-Fernández, A.; Marcos-Cives, I.; Platas-Iglesias, C.; Castro-García, S.; Sánchez-Andújar, M. Diimidazolium Halobismuthates [Dim]₂[Bi₂X₁₀] (X = Cl-, Br-, or I-): A New Class of Thermochromic and Photoluminescent Materials. *Inorg. Chem.* **2018**, *57* (13), 7655–7664. <https://doi.org/10.1021/acs.inorgchem.8b00629>.
- (4) Diniz, J. R.; De Lima, T. B.; Galaverna, R.; De Oliveira, A. L.; Ferreira, D. A. C.; Gozzo, F. C.; Eberlin, M. N.; Dupont, J.; Neto, B. A. D. Is the Formation of N-Heterocyclic Carbenes (NHCs) a Feasible Mechanism for the Distillation of Imidazolium Ionic Liquids? *Phys. Chem. Chem. Phys.* **2018**, *20* (38), 24716–24725. <https://doi.org/10.1039/c8cp03609h>.
- (5) Godajdar, B. M.; Kiasat, A. R.; Hashemi, M. M. Synthesis, Characterization and Application of Magnetic Room Temperature Dicationic Ionic Liquid as an Efficient Catalyst for the Preparation of 1,2-Azidoalcohols. *J. Mol. Liq.* **2013**, *183*, 14–19. <https://doi.org/10.1016/j.molliq.2013.03.022>.
- (6) Cassol, C. C.; Ebeling, G.; Ferrera, B.; Dupont, J. A Simple and Practical Method for the Preparation and Purity Determination of Halide-Free Imidazolium Ionic Liquids. *Adv. Synth. Catal.* **2006**, *348* (1–2), 243–248. <https://doi.org/10.1002/adsc.200505295>.
- (7) Aher, S. B.; Bhagat, P. R. Convenient Synthesis of Imidazolium Based Dicationic Ionic Liquids. *Res. Chem. Intermed.* **2016**, *42* (6), 5587–5596. <https://doi.org/10.1007/s11164-015-2388-4>.
- (8) Rountree, E. S.; McCarthy, B. D.; Eisenhart, T. T.; Dempsey, J. L. Evaluation of Homogeneous Electrocatalysts by Cyclic Voltammetry. *Inorg. Chem.* **2014**, *53* (19), 9983–10002. <https://doi.org/10.1021/ic500658x>.
- (9) Kosugi, K.; Kondo, M.; Masaoka, S. Quick and Easy Method to Dramatically Improve the Electrochemical CO₂ Reduction Activity of an Iron Porphyrin Complex. *Angew. Chem. Int. Ed.*

2021, *133* (40), 22241–22245. <https://doi.org/10.1002/ange.202110190>.

- (10) Savéant, J.-M. Evidence for Concerted Pathways in Ion-Pairing Coupled Electron Transfers. *J. Am. Chem. Soc.* **2008**, *130* (14), 4732–4741. <https://doi.org/10.1021/ja077480f>.
- (11) Jensen, M. T.; Rønne, M. H.; Ravn, A. K.; Juhl, R. W.; Nielsen, D. U.; Hu, X.-M.; Pedersen, S. U.; Daasbjerg, K.; Skrydstrup, T. Scalable Carbon Dioxide Electroreduction Coupled to Carbonylation Chemistry. *Nat. Commun.* **2017**, *8* (489), 489. <https://doi.org/10.1038/s41467-017-00559-8>.
- (12) Fukuyama, T.; Mukai, Y.; Skrydstrup, T.; Ryu, I. Modernized Low Pressure Carbonylation Methods in Batch and Flow Employing Common Acids as a CO Source. *Org. Lett.* **2013**, *15*, 2794–2797. [https://doi.org/10.1002/047084289X.rc013.pub2.\(2\)](https://doi.org/10.1002/047084289X.rc013.pub2.(2)).
- (13) Khedkar, M. V.; Sasaki, T.; Bhanage, B. M. Immobilized Palladium Metal-Containing Ionic Liquid-Catalyzed Alkoxy carbonylation, Phenoxy carbonylation, and Aminocarbonylation Reactions. *ACS Catal.* **2013**, *3*, 287–293.